AD-A048 868 NAVAL UNDERSEA WARFARE CENTER SAN DIEGO CALIF F/G 20/1
STUDY OF EFFECT OF SEDIMENT SHEAR WAVES ON BOTTOM REFLECTION LO--ETC(U)
DEC 67 H E MORRIS

UNCLASSIFIED NUWC-TN-7 NL

| OF |

AD
A048868

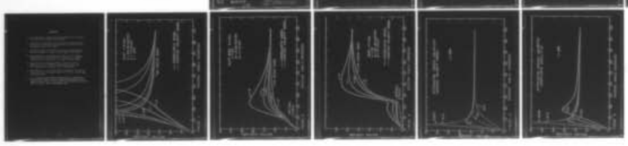

END
DATE
FILMED
2-78
DDC

MOST Project-2

NUWC TN 7

NAVAL UNDERSEA WARFARE CENTER

DECEMBER 1967

14 NUWC-TN-7

6

STUDY OF EFFECT OF SEDIMENT SHEAR WAVES ON BOTTOM REFLECTION LOSSES IN UNDERWATER ACOUSTICS,

10 by H.E. Morris
San Diego, California

11 Dec 67

SUBPROJECT NO. SF1010315

~~TASK NO. 6105~~

DISTRIBUTION STATEMENT A
Approved for public release;
Distribution Unlimited

12 18p.

16 F10103

17 SF1010315

TN 7

403023

001503

A series of bottom reflection losses are presented in graphical form to show the contribution of shear waves when included in the theoretical acoustic model for bottom sediments. The analysis illustrates the effect of introducing shear waves in the more complicated theoretical model for viscoelastic solids. This memorandum has been prepared because it is believed that the information may be useful in this form to others at NUWC and to a few persons outside NUWC. This memorandum should not be construed as a report since its only function is to present limited supplementary information on previously published theoretical work.

INTRODUCTION *

During the last twenty years models of the bottom sediments for use in the calculation of reflection loss have become increasingly complex. The simple impedance model and the Rayleigh liquid model frequently predict inaccurate values of loss. Corrections to the Rayleigh liquid model have been made by Mackenzie,[1] and Bell[2] and Cole[3] by assuming the sound velocity to be a complex number with the imaginary part of the velocity related to sound attenuation in the sediment. The new complex velocity model resulted in increased values of calculated bottom reflection loss and better general agreement with experimental values, but neglected the shear waves that would be generated in the sediment. Since the attenuation of sound in sediments was not accurately known, the attenuation for the complex velocity model could be chosen for a fit of calculated and experimental values of "bottom loss", and without regard for the actual attenuation in the sediment.

A more accurate model of the sediments is that of a viscoelastic material. Here the sediment properties are defined by the complex Lamé constants. Shear waves are generated as a result of both the sediment rigidity (related to the real part of μ) and the sediment viscosity (related to the imaginary parts of μ and λ).

The purpose of this memorandum is to compare the results of the complex velocity liquid model with the viscoelastic model where the same density, compressional velocity, and attenuation in the sediments are used for both models. Knowledge of sediments and acoustic measurements sensitive to the differences between these two models can then be used to gain a better understanding of both attenuation and reflection.

---

* Information from this memorandum was presented as Paper T10 at the 74th Meeting of the Acoustical Society of America, Miami Beach, Florida, 13-17 November 1967. Work was accomplished under NAVSHIPS Subproject SF101-03-15 Task 8105.

MATHEMATICAL ANALYSIS

Equations for the bottom loss as developed by Bucker[4,5] are for a layered viscoelastic solid model. To compare such a theoretical viscoelastic model with work by Cole[3] and Barnard, et al,[6] the bottom losses for a complex velocity model were calculated using the following mathematical derivations for a water layer of constant velocity and an underlying sediment half-space with absorption.

The problem of the reflection of a plane sound wave at a plane boundary separating two media, Fig. A, has a solution for the incident, reflected, and transmitted waves in the following forms.

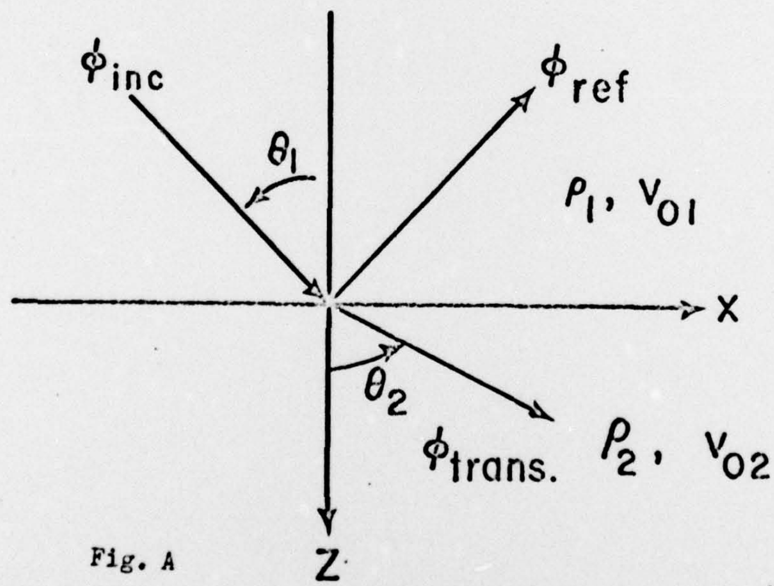

Fig. A

$$\phi\ inc = A \exp i\ (k_1\ z \cos\theta_1 + k_1\ x \sin\theta_1 - \omega t)$$

$$\phi\ ref = R \exp i\ (- k_1\ z \cos\theta_1 + k_1\ x \sin\theta_1 - \omega t)$$

$$\phi\ trans = T \exp i\ (k_2\ z \cos\theta_2 + k_2\ x \sin\theta_2 - \omega t)$$

Let $k^* \equiv k_1 \sin \theta_1 \equiv k_2 \sin \theta_2$ (by Snell's Law) and $k^* a_1 \equiv k_1 \cos \theta_1$,

$\therefore a_1 = \cot \theta_1$.

Then $\phi\ inc = A \exp i\ (k^* a_1 z + k^* x - \omega t)$

$\phi\ ref = R \exp i\ (-k^* a_1 z + k^* x - \omega t)$

$\phi\ trans = T \exp i\ (k^* a_2 z + k^* x - \omega t)$.

The boundary conditions at the interface are that there is continuity of the vertical component of velocity and continuity of pressure.

Thus $\partial \phi_1 / \partial z = \partial \phi_2 / \partial z$,

and $\rho_1\ \partial \phi_1/\partial t = \rho_2\ \partial \phi_2/\partial t$ at $z = 0$.

Then $R = \dfrac{a_1 \rho_2 - a_2 \rho_1}{a_1 \rho_2 + a_2 \rho_1}$, $\quad T = \dfrac{2 a_1 \rho_1}{a_1 \rho_2 + a_2 \rho_1}$

Here R is the reflection coefficient and T is the transmission coefficient.

Values of a_1 and a_2 are determined by the angle of the incident wave and the requirement that the velocity potentials satisfy the wave equation. This means that

$$k^* = \omega \sin \theta_1 / v_{01}, \therefore a_1 = \cot \theta_1.$$

Also, $\nabla^2 \phi_2 = \dfrac{1}{v_2^2} \dfrac{\partial^2 \phi_2}{\partial t^2}$ (the wave equation)

Therefore, $k^{*2} a_2^2 + k^{*2} = \omega^2/v_2^2$.

Absorption will be introduced into the solution by making a_2 complex. Consider a plane wave traveling in the plus z direction in medium 2.

This wave will have the form

$$\exp i\,(\xi\, z - \omega t)$$

where $\xi = \omega/v_2$ from the wave equation.

Let $\xi = \xi' + i\,\xi''$, then the wave has the form

$$\exp\,(i\,\xi'\, z - \omega t)\,\exp\,(-\,\xi''\, z).$$

Thus ξ' is equal to ω/v_{02} where v_{02} is the measured sediment velocity and ξ'' is equal to α_2, the measured attenuation in nepers/unit-length.

It follows that

$$v_2 = \frac{\omega^2\, v_{02} - i\,\omega\,\alpha_2\, v_{02}^2}{\omega^2 + \alpha_2^2\, v_{02}^2}$$

and $a_2^2 = c^2/v_2^2 - 1$

where c = horizontal phase velocity = ω/k^* .

The root of a_2^2 used in the calculations corresponds to a wave attenuated in the z direction.

PHYSICAL MODELS

Three hypothetical physical cases representing clay, silty-sand, and sand were considered in this study. The same densities, compressional velocities, and attenuations in the sediment were used for both theoretical approaches, the complex velocity model and the visco-elastic model. Bottom loss curves were calculated for several frequencies in the low kHz region with similar results. Only curves for 3.5 kHz are shown in this memorandum.

TABLE I: BOTTOM CONSTANTS

	Velocity (m/sec)	Velocity Ratio η^*	Atten(db/m) 3.5 kHz	Density g/cm^3
WATER	1530			1.03
CLAY	1484	.970	.84	1.4
SILTY-SAND	1561	1.02	1.8	1.7
SAND	1701	1.12	1.116	1.9

$$\eta^* = \frac{\text{sediment velocity}}{\text{water velocity}}$$

SHEAR WAVES

Shear waves have been found to exist in marine sediments. Shear waves were measured "in situ" by Bucker in shallow water and to 3500 ft. depth on the continental shelf. He found measurable shear velocities in mud as well as sand. High shear velocities of approximately 260 meters/sec for deep sea clays have been measured by Hamilton [7] on stations of two recent cruises in the Pacific. To correspond to a rigorous theoretical examination of bottom reflection loss, shear waves would necessarily need to be included.

Rigidity of the sediment is introduced in the theoretical viscoelastic solid model by the ratio, $Re\,\mu/Re\,\lambda$ [4]. This is equivalent to specifying Poisson's ratio for the sediment layer. It should be noted that when $Re\,\mu/Re\,\lambda = 0$, some effect of the shear waves is still present from the contribution of $Im\,\mu$ related to viscosity. Cases were computed for ratios of 0, 0.01, 0.03, 0.1, and 0.2. These ratios are equivalent to specifying a range of Poisson's ratio from 0.5 to 0.417.

RESULTS

The bottom loss was calculated for two models, both of which consisted of a water layer overlying a sediment half-space. Velocity and attenuation selections varied the sediment from clay to silty-sand to sand. Varying amounts of rigidity, $r = Re\mu/Re\lambda$, were introduced into the sediment layer. The results are shown in figures 1 to 3. As seen in the graphs, consideration of the shear waves has a decided effect on bottom loss and is most obvious for silty-sand. Increasing the rigidity increased the bottom loss.

The dashed lines labeled "no shear" represent the complex velocity, or absorbing liquid, model. When the ratio r is zero there is still discrepancy between the two curves, indicating the contribution of the imaginary part of μ , which may be significant even in this case when the two models are most nearly alike. As the number of sediment layers increases beyond the single sediment half-space a more decisive difference than illustrated here would be expected in the results.

Figure 1 shows bottom reflection loss plotted versus grazing angle for a low-velocity bottom. Both models result in "intromission" losses and there is a shifting of the high-loss angular region as "r" is increased in the visco-elastic model. Note, however, that the result for r = 0.03 would be similar to the "no shear wave" model. Plots for r = 0.1 and 0.2 are not realistic for clay but are included here for completeness.

Figure 2 is a silty-sand case. The sound velocity ratio of sound velocities in sediment and water for η slightly $>$ 1, the attenuation and density are typical of silty-sand bottom sediments. Increasing the r ratio greatly increased the bottom loss from 20 to 30 degrees. From sea-floor data[7], r ratios from 0.1 to 0.2 seem to be reasonable for sediments of this velocity and density.

Figure 3 represents a "fast bottom" case of sand. Notice a change of scale on bottom loss. With no attenuation one would have the Rayleigh case. The Rayleigh form seems recognizable here, but with an added loss as the critical angle is approached. This probably indicates that attenuation is not as important here to the shape of the curve as for the low-velocity case in Figure 1.

The "r" ratios from measurements tend to run 0.2 and above. In this case, r = 0.03 and 0.1 should not be considered realistic; and even higher values of bottom loss might be calculated and observed. The difference in models near 40 and 50 degrees seems to be measurable and suggests further experiments.

Figures 4 and 5 illustrate changes of attenuation α in sediments. Both treat a constant "low velocity" bottom where η is slightly < 1 which is appropriate for some clays.

Figure 4 shows the effect on bottom loss for the complex velocity model when the velocity was held constant and the attenuation values were varied from 0 to 10 db/meter. There was less bottom loss with increased attenuation. It should be noted that for low-velocity liquid sediments the angle of intromission occurs when $a_1 \rho_2 = a_2 \rho_1$ as can be seen from the equation for the reflection coefficient. For sediments with attenuation this condition cannot be satisfied as a_2 will be complex.

Figure 5 shows the effect of the same increases of attenuation for the visco-elastic model when r = 0. As the sediment attenuation increases, the bottom losses at first become less near the angle of intromission in this model. However, with further increasing attenuation in this visco-elastic model a peak in the bottom loss curve will eventually build up as shown for α = 10. This reappearance of a peak loss is due to the attenuation of shear waves in the sediment. Although the real part of $\mu = 0$, there is a contribution from the imaginary part of μ . This peak, though occurring at a very high attenuation for our purpose, does show the effect of shear attenuation in a highly viscous material.

CONCLUSION

An effort was made to select three representative sea-floor types. In all cases the introduction of shear waves resulted in higher-theoretical bottom reflection losses. For the case of the shear-wave model with zero rigidity bottom reflection loss was very close to the "no shear" model. For non-zero rigidity and reasonable ranges of "r" ratios we feel that the results definitely are not the same for cases of interest and for the two types of models. It is believed that at least a few important sea-floor areas do exhibit these rigidity ratios, and that for a rigorous, accurate treatment the shear waves should be included in the theoretical model.

Also, these calculations imply that for normal incidence reflection there is not much difference for either model or for any of the sediments investigated. For sands, and grazing angles 30 to 50 degrees, there should be measurable losses that might be used to demonstrate differences between models.

REFERENCES

1. K. V. Mackenzie, "Reflection of Sound from Coastal Bottoms," J. Acoust. Soc. Am. 32, 221-229 (1960).

2. H. W. Marsh, T. G. Bell, and C. W. Horton, "Reflection and Scattering of Sound by the Sea Bottom", Acoustical Soc. of Am. meeting, Oct. 21-24, 1964.

3. B. F. Cole, "Marine Sediment Attenuation and Ocean-Bottom-Reflected Sound", J. Acoust. Soc. Am. 38, 291-297 (1965).

4. H. P. Bucker, J. A. Whitney, G. S. Yee, and R. R. Gardner, "Reflection of Low-Frequency Sonar Signals from a Smooth Ocean Bottom", J. Acoust. Soc. Am. 37, 1037-1051 (1965).

5. Navy Electronics Laboratory Technical Report, "Bottom Reflection Losses: FASOR I", by Halcyon E. Morris and H. P. Bucker, Research Report 1360, 7 March 1966

6. G. R. Barnard, J. L. Bardin, and W. B. Hempkins, "Underwater Sound Reflection from Layered Media", J. Acoust. Soc. Am. 36, 2119-2123 (1964).

7. E. L. Hamilton, Naval Undersea Warfare Center, "Predictions of Sea Floor Sediment Acoustic Properties and Models, North Pacific", Paper 2D6, 24th Navy Symposium on Underwater Acoustics, Nov 29 to Dec 1, 1966, Philadelphia, Penn.

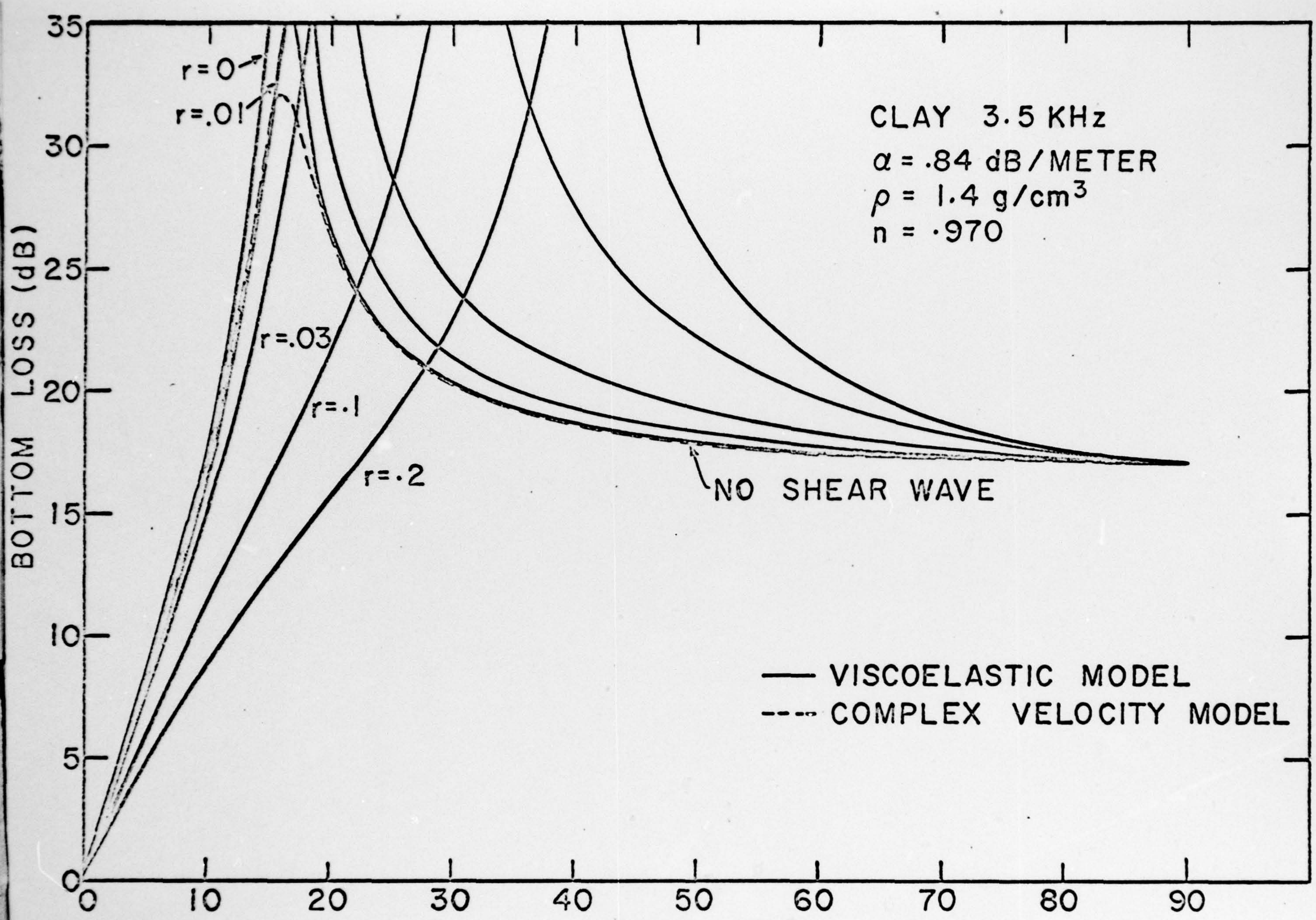

BOTTOM LOSS (dB)
GRAZING ANGLE (DEGREES)
r=0
r=.01
r=.03
r=.1
r=.2
NO SHEAR WAVE
CLAY 3.5 KHz
α = .84 dB/METER
ρ = 1.4 g/cm³
n = .970
VISCOELASTIC MODEL
COMPLEX VELOCITY MODEL

FIGURE 1

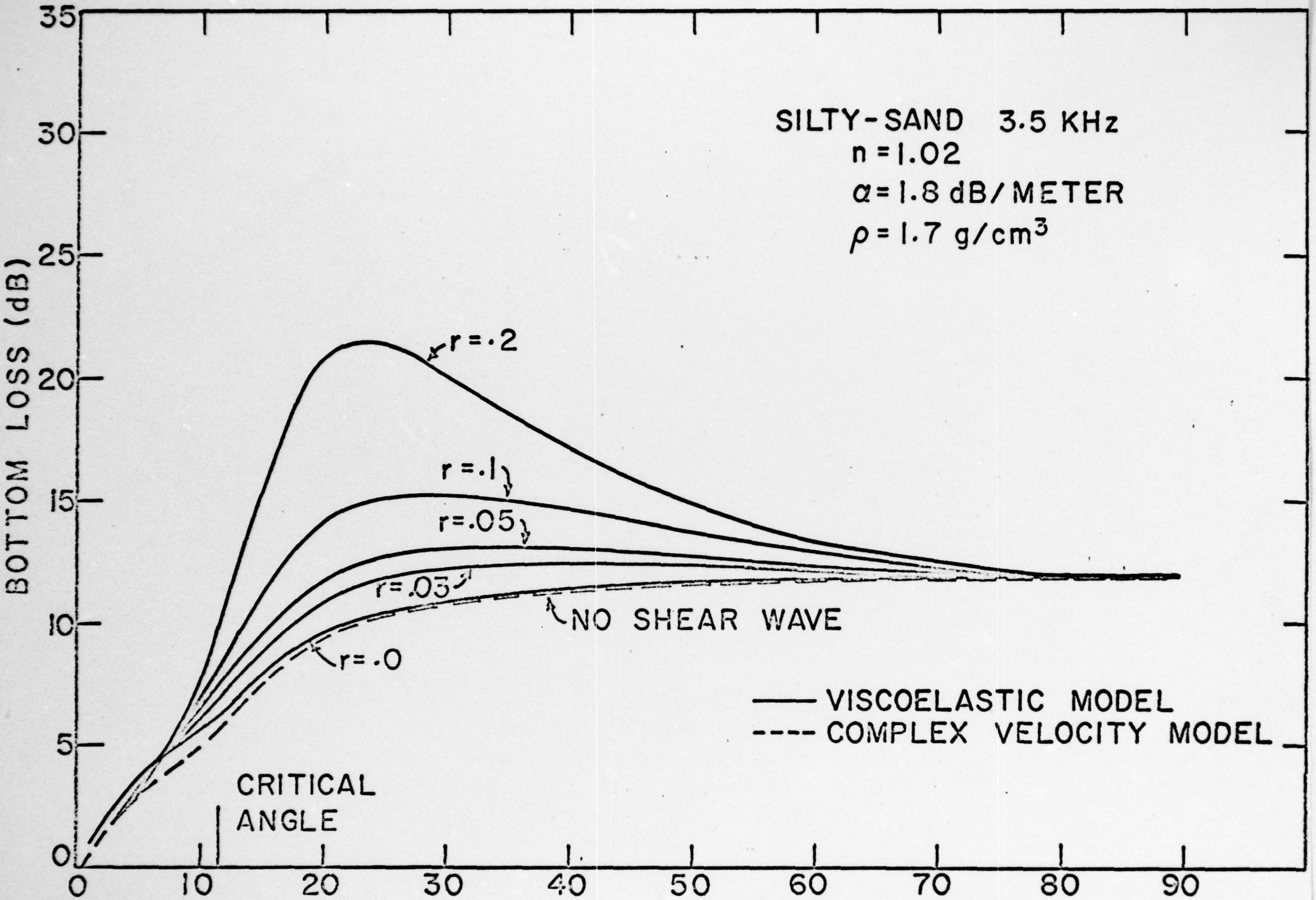
SILTY-SAND 3.5 KHz
n = 1.02
α = 1.8 dB/METER
ρ = 1.7 g/cm3
r = .2
r = .1
r = .05
r = .03
r = .0
NO SHEAR WAVE
CRITICAL ANGLE
VISCOELASTIC MODEL
COMPLEX VELOCITY MODEL
BOTTOM LOSS (dB)
GRAZING ANGLE (DEGREES)
0
5
10
15
20
25
30
35
0
10
20
30
40
50
60
70
80
90

FIGURE 2

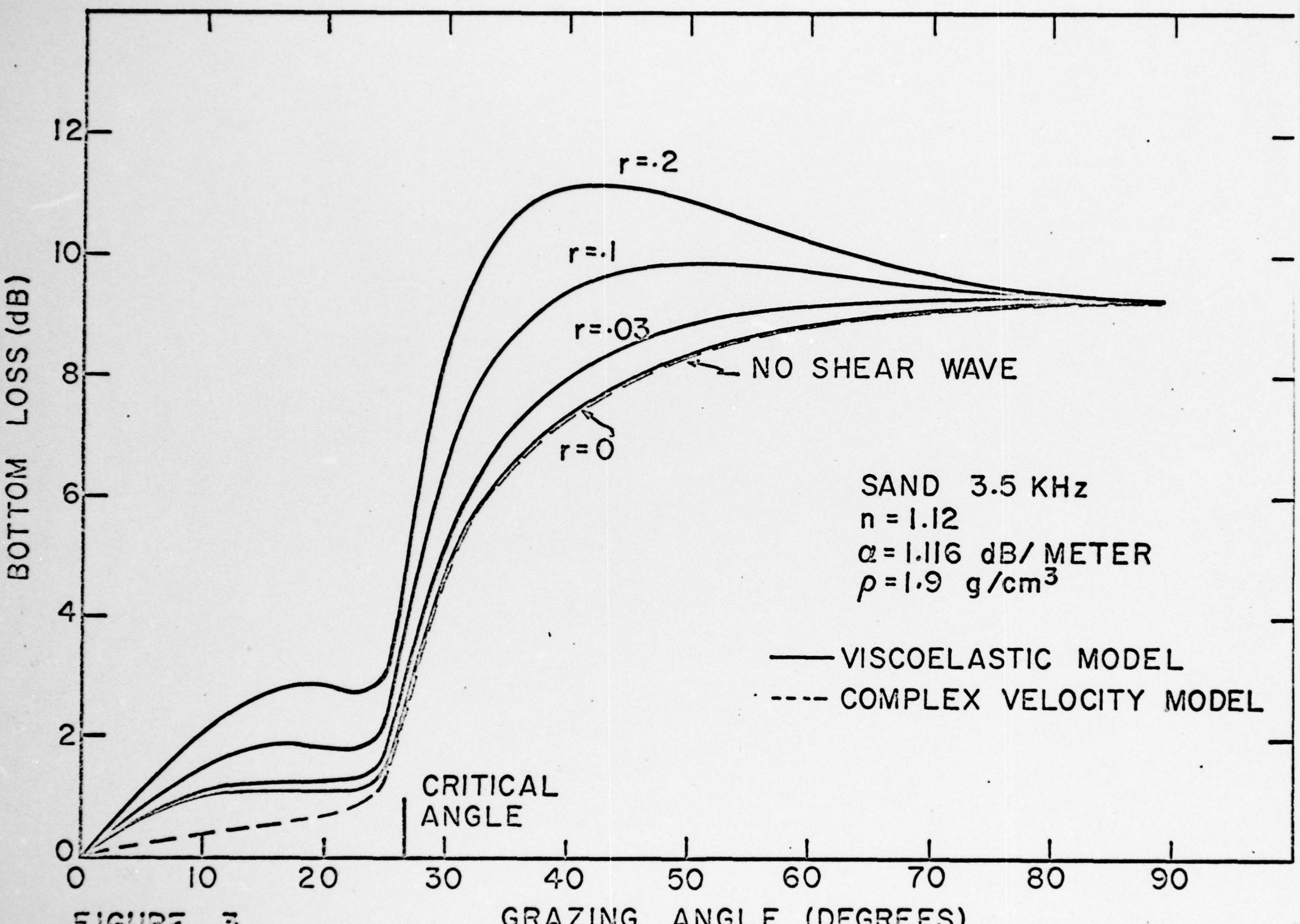
BOTTOM LOSS (dB)
0
2
4
6
8
10
12
GRAZING ANGLE (DEGREES)
0
10
20
30
40
50
60
70
80
90
r=.2
r=.1
r=.03
r=0
NO SHEAR WAVE
CRITICAL ANGLE
SAND 3.5 KHz
n = 1.12
α = 1.116 dB/ METER
ρ = 1.9 g/cm3
VISCOELASTIC MODEL
COMPLEX VELOCITY MODEL

FIGURE 3

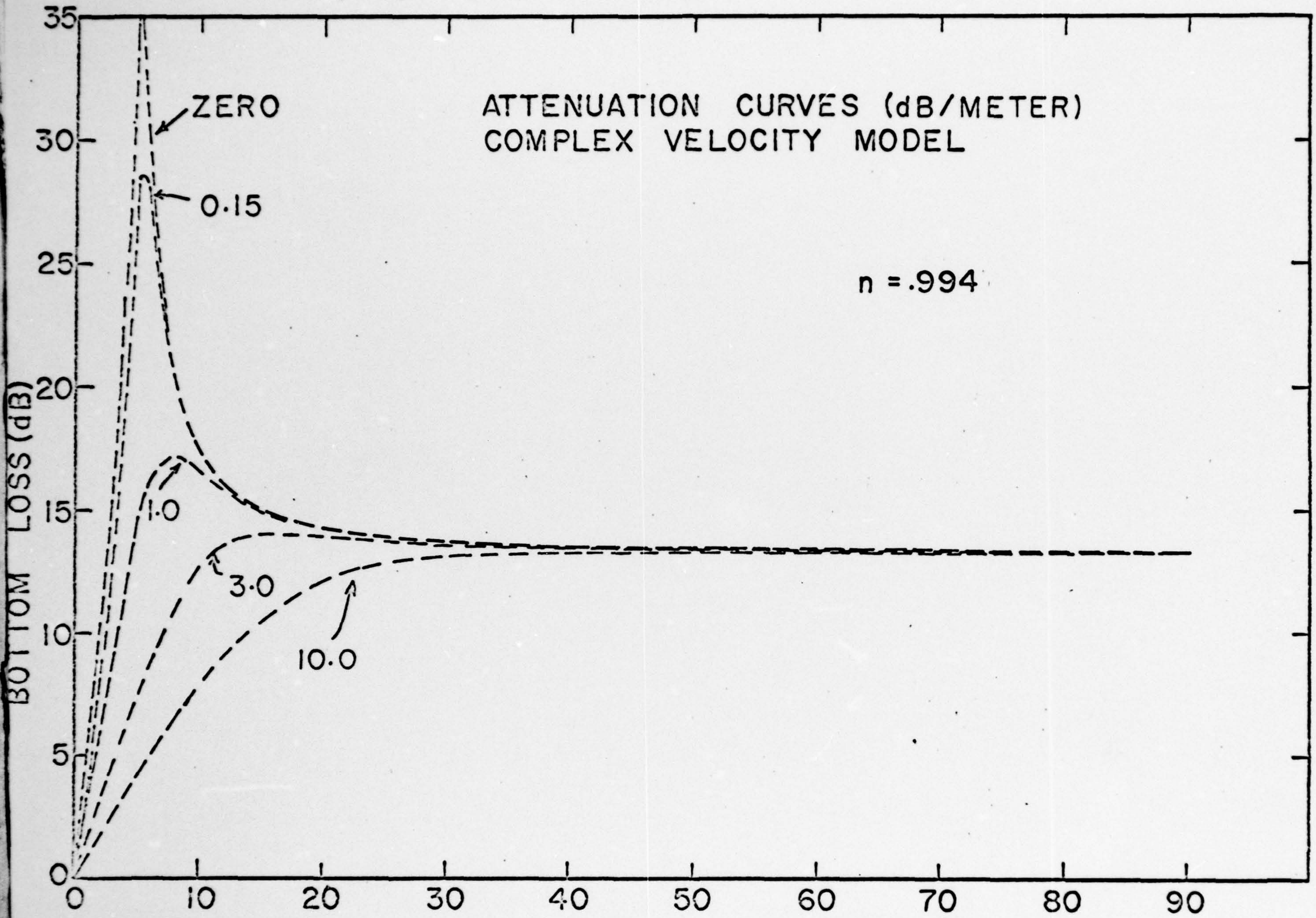

ATTENUATION CURVES (dB/METER)
COMPLEX VELOCITY MODEL
n = .994
ZERO
0.15
1.0
3.0
10.0
BOTTOM LOSS (dB)
GRAZING ANGLE (DEGREES)
0
5
10
15
20
25
30
35
0
10
20
30
40
50
60
70
80
90

FIGURE 4

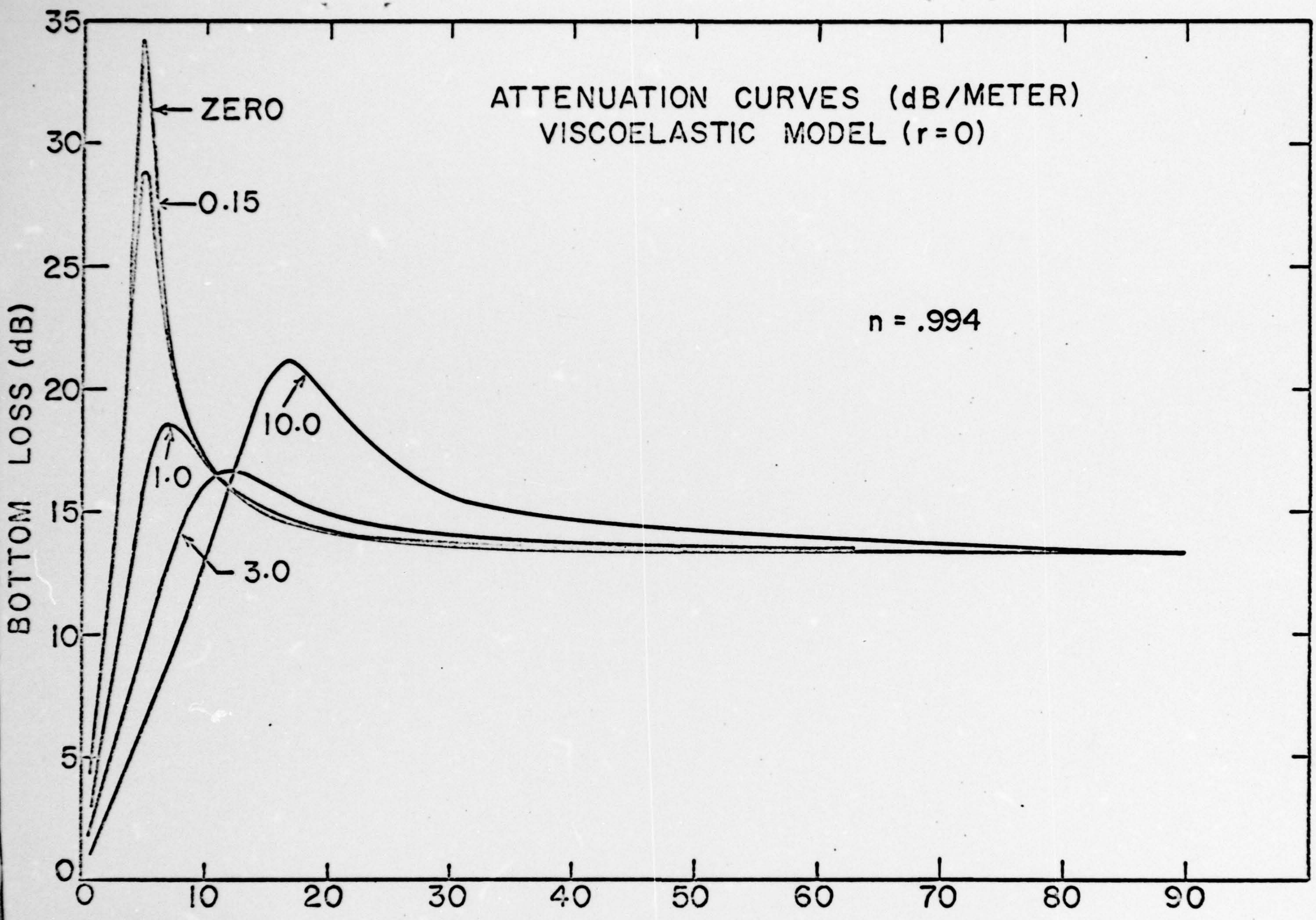

ATTENUATION CURVES (dB/METER)
VISCOELASTIC MODEL (r=0)
n = .994
ZERO
0.15
1.0
3.0
10.0
BOTTOM LOSS (dB)
0
5
10
15
20
25
30
35
0
10
20
30
40
50
60
70
80
90
GRAZING ANGLE (DEGREES)

FIGURE 5